A FIELD STUDY ON THE CHARACTERISTICS OF AIR BUBBLE PLUME IN A RESERVOIR

By

Shiro Matsunashi

Research Engineer, Environmental Hydraulics Section, Abiko
Research Laboratory, Central Research Institute of Electric Power Industry

and

Yoichi Miyanaga

Manager, Environmental Hydraulics Section, Abiko Research Laboratory,
Central Research Institute of Electric Power Industry

SYNOPSIS

Mixing of reservoirs and lakes by air bubble plumes has been proposed as a measure for the improvement of water quality. In this study, properties of the air bubbles, the flow induced by air release and the resulting destratification are investigated experimentally in an existing reservoir. The following results were obtained.

1. The measured bubble diameter ranged from 5 to 7mm.
2. The measured bubble rising speed ranged from 50 to 150cm/s. It can be expressed as a function of air supply rate.
3. The measured volume flux ratio of the water to the air can be explained partly by an integral theory for bubble plumes in a homogeneous environment. However, the theory overestimates the volume flux ratio for the data with a plume height greater than 20m. This is attributable to the stratification of the ambient water.

INTRODUCTION

Mixing of reservoirs and lakes by air bubble plumes has been proposed as a measure for the improvement of water quality. Studies on the effect of this method have been carried out both in the field and in the laboratory by the Ministry of Construction, etc. in Japan. However, the hydraulic design for this method has not been established since the information with regard to the basic properties of air bubble plumes, the entrainment flux and the destratification mechanism is inadequate.

The authors have studied the relationship between the condition of air supply and the basic properties of air-bubble plumes (3). Based on the relationship, a flow model taking into account the underwater air release in a reservoir (4) has been developed. Combined with the theoretical background for the improvement of water quality by an artificial mixing (5), the model has been applied to predict the effect of air bubble method. In order to extend this model to prototype reservoirs of various scales, it is necessary to examine the bubble rising speed and the entrainment flux further in detail.

This study examines the properties of air bubble plumes by a field experiment in comparison with our previous laboratory experiments (3).
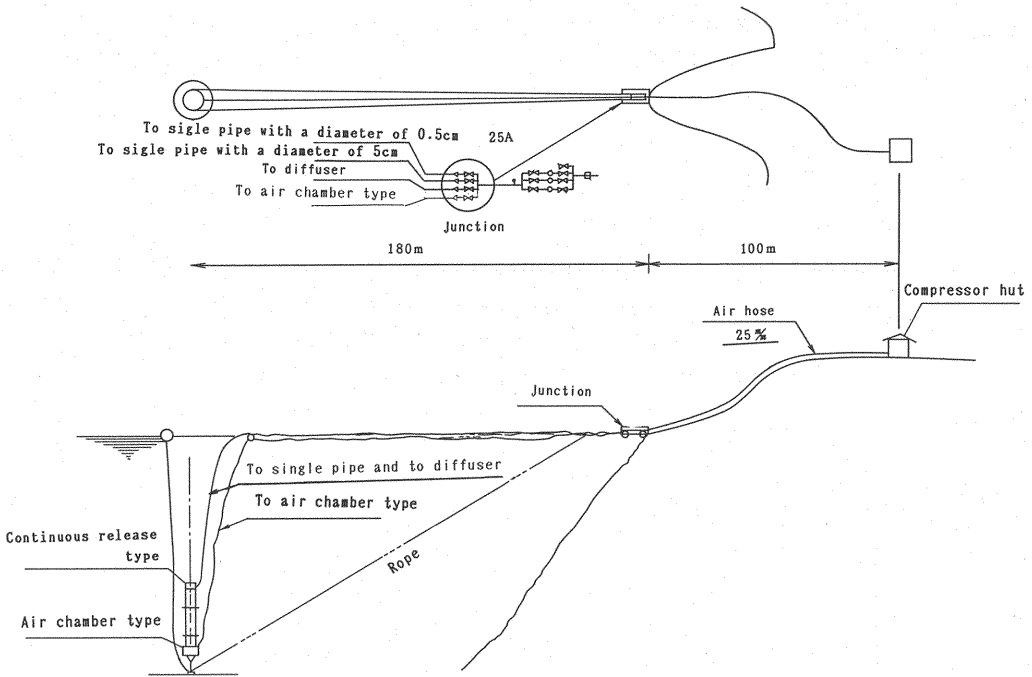
EXPERIMENTAL METHOD

Fig. 1 Air release and supply equipment

Table 1 Air release equipment

Method of mixture	Air supply equipment		Material
Continuous release type	Single pipe	diameter is 0.5cm	Vinyl chloride
		diameter is 5cm	
	Diffuser Duffuser diameter is 50cm Hole diameter is 0.5cm There are 100 holes on the diffuser		
Air chamber type	Air chamber type Diameter is 50cm Cylinder length is 10m Air chamber volume is 78.74 liter		FRP

Experiments were performed at a reservoir with a volume of 338,400,000m^3 and a total depth of 80m. The experimental equipment was shown schematically in Fig. 1. Air was supplied from the compressor on the land to three types of air release equipment : (i) single pipe, (ii) diffuser and (iii) air chamber type. Characteristics of air release equipment are summarized in Table 1. The type of air release was chozen and the rate of air supply was controlled at the junction. Air release equipment was installed about 180m off the shoreline and the depth of air release was changeable. Depths of 20 and 30m were chosen in the measurement.

The experiments consist of air bubble and plume measurements. Shape, dia- meter and rising speed of bubbles were measured by photographs with a distance of from 1 to 4m vertically and were statistically averaged at each depth. The vertical velocity distribution in a plume was measured by electromagnetic current meters for three components of velocity, and the temperature distribution by a
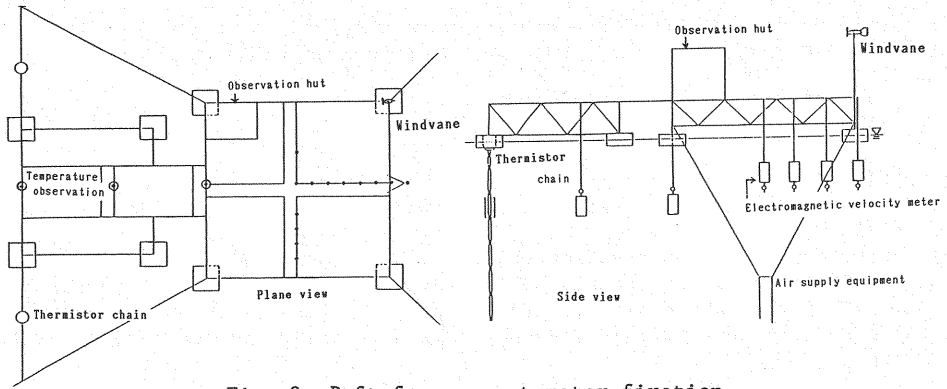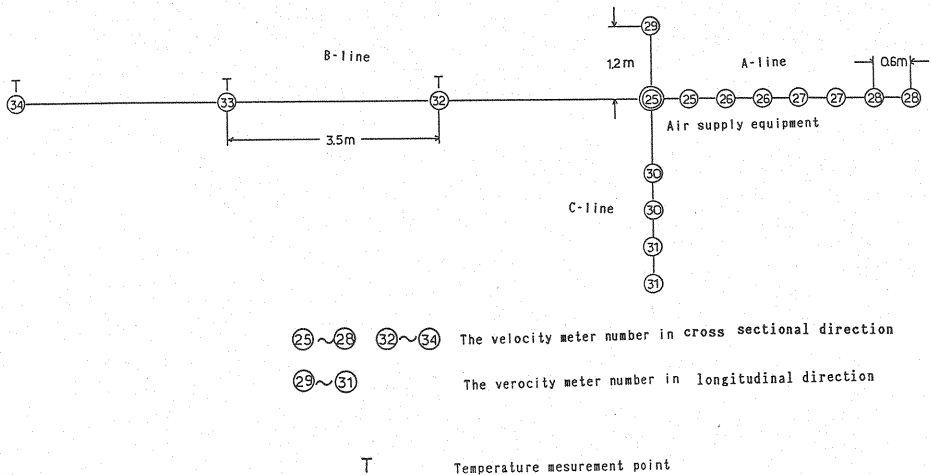
Fig. 2   Raft for current meter fixation

Fig. 3   Measurement points of velocity

thermistor sensor. Current meters were supported in the reservoir by being hung
from a raft which was moored to four anchors. The raft for current meter fixation
is shown in Figs. 2 and 3. The current meters were installed horizontally at a
certain depth with an interval of 1.2m and were moved in the horizontal direction
by 0.6m for fitting each measuring point. Therefore each current meter was not
influenced by the magnetic fields of the other current meters. The plume velocity
was measured for 7 minutes with an interval of 0.5 second at one measuring point
and averaged in each measurement period. In the case of an intermittent air
release (air chamber type), the maximum value of the period of air release was
50 seconds. Thus the data of at least 7 periods were obtained.
    During the experiment the change in the temperature stratification of the
ambient water was negligible.

RESULTS AND DISCUSSION

Characteristics of bubbles

    Classification of the shape of bubbles is shown in Table 2 (2). A lot of
sphere bubbles were observed in the author's previous laboratory experiments. In
the present field experiments, the Reynolds number of bubbles was 3000~9000 and a

lot of spheroid and mushroom-shape bubbles were observed.

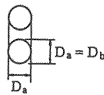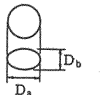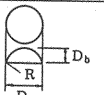The Reynolds number of the bubble Re is defined as follows.

$$Re = \frac{d\,Wa}{\nu} \tag{1}$$

Examples of the change in bubble diameter with the height above the air outlet and with air supply rates are shown in Figs. 4 and 5. The bubble diameter ranges from 5 to 7mm.

A theoretical equation based on the balance of buoyancy force and surface tension of single bubble at the air outlet (3) predicts the bubble diameter from 6 to 13mm. Thus the bubble diameter for large air supply rate can be approximately estimated from the theory of single bubble which is valid for the case of small air supply rate.

Table 2　Calculation of bubble characteristics

Shape of bubble	Bubble of sphere	Spheroid	Mushroom-shape
Size of bubble	less than 0.2cm	0.2~1.8 cm	more than 1.8cm
Reynolds number of bubble	$Re < 1$	$1 < Re < 5000$	$5000 < Re$
Image	$D_a = D_b$, D_a	D_b, D_a	D_b, R, D_a
Volume	$V = \frac{\pi}{6}Da^3 = \frac{\pi}{6}d^3$	$V = \frac{\pi}{6}Da^2 \cdot D_b = \frac{\pi}{6}d^3$	$V = \frac{\pi D_b{}^2}{3}(3R - D_b)$ $= \frac{\pi D_b}{24}(3\,Da^2 + 4\,D_b{}^2)$
Equivalent sphere diameter	$d = Da = D_b$	$d = (Da^2 \cdot D_b)^{1/3}$	$d = (\frac{Da}{4}(3\,Da^2 + 4\,D_b{}^2))^{1/3}$

Symbol	Pattern No.	Air release equipment	Air release depth (m)	Air supply (cm³/s)
▼	0 5	Diffuser	2 0	2 5 5 0
■	0 6	"	2 0	6 2 0 0
●	0 7	"	2 0	1 2 0 0 0
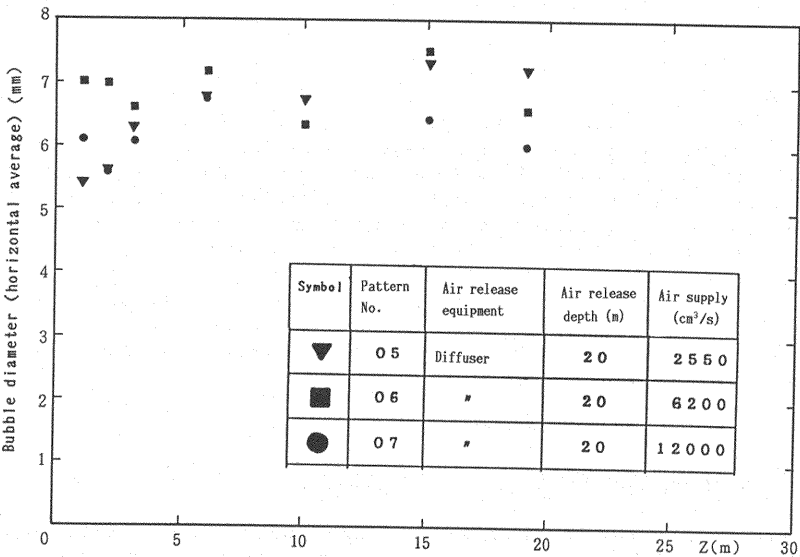
Fig. 4　Vertical distribution of bubble diameter

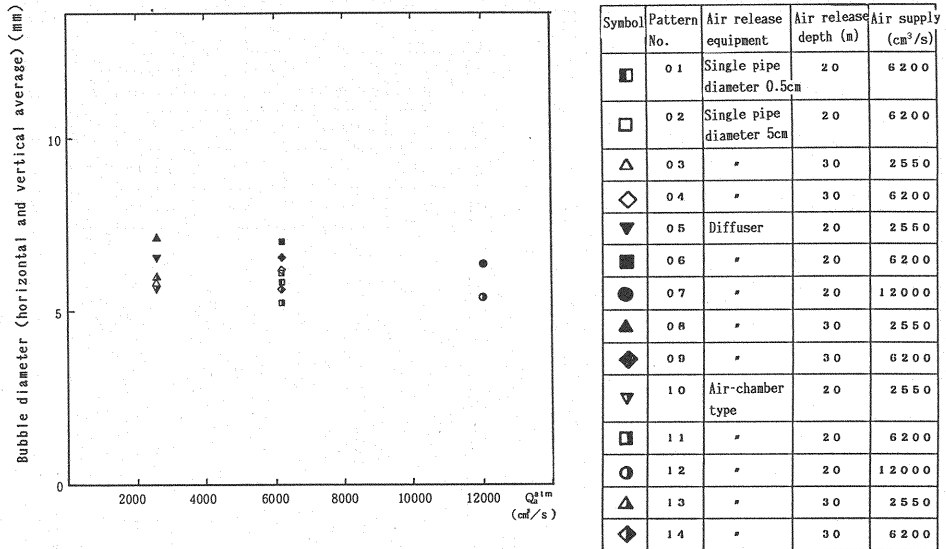| Symbol	Pattern No.	Air release equipment	Air release depth (m)	Air supply (cm³/s)
▣	01	Single pipe diameter 0.5cm	20	6200
□	02	Single pipe diameter 5cm	20	6200
△	03	"	30	2550
◇	04	"	30	6200
▼	05	Diffuser	20	2550
■	06	"	20	6200
●	07	"	20	12000
▲	08	"	30	2550
◆	09	"	30	6200
▽	10	Air-chamber type	20	2550
◫	11	"	20	6200
◐	12	"	20	12000
△	13	"	30	2550
◈	14	"	30	6200

Fig. 5   Relationship between bubble diameter and air supply

Examples of the change in bubble rising speed with the height above the air outlet and with air supply rate are shown in Figs. 6 and 7. The bubble rising speed ranges from 50 to 150 cm/s. It decreases with height and increases with air supply rate.

Tadaki and Maeda (6) presented the following relationships between the Reynolds number of the bubble and the drag coefficient Cd.

$$\left.\begin{array}{ll} Cd = 2.6 & \text{when } 4483.7 \leqq Re \\[2mm] Cd = 0.29\ Re^{0.26} & \text{when } 1630.4 \leqq Re \leqq 4483.7 \\[2mm] Cd = 2.82*10^{-6} Re^{1.82} & \text{when } 414.7 \leqq Re \leqq 1630.4 \end{array}\right\} \qquad (2)$$

The authors have shown that for small air supply rate, the bubble rising speed can be estimated from a theory for single bubble (3) based on the balance of buoyancy and drag force which is calculated from equation (2). However for the case of large air supply rate such as the present field experiments, the theory is not applicable to the estimation of the bubble rising speed. Therefore the following recursive equation can be applied for practical use based on the experimental data of the authors and Kobus (1) as shown in Fig. 7.

$$Wa = 11.3\ Qa^{atm1/4} \qquad (3)$$

Characteristics of air bubble plume

During the field experiments, temperature distribution of the ambient water did not change significantly as shown in Figs. 8 and 9. Therefore, the entrainment of the ambient water by air bubble plumes in the stratified environment can be analysed assuming that the stratification did not change.

The horizontal velocity profiles near the surface is shown in Figs. 10 and 11. Near the bubble column the flow below the depth of 0.6m was directed towards the bubble column, and the flow above this depth was spread radially in a very thin surface layer. Far from the bubble column the surface flow diffused and submerged owing to the relative density difference from the ambient water.

The horizontal distributions of vertical plume velocity can be approximated as Gaussian. The half widths of profiles of plume velocity, air bubbles and
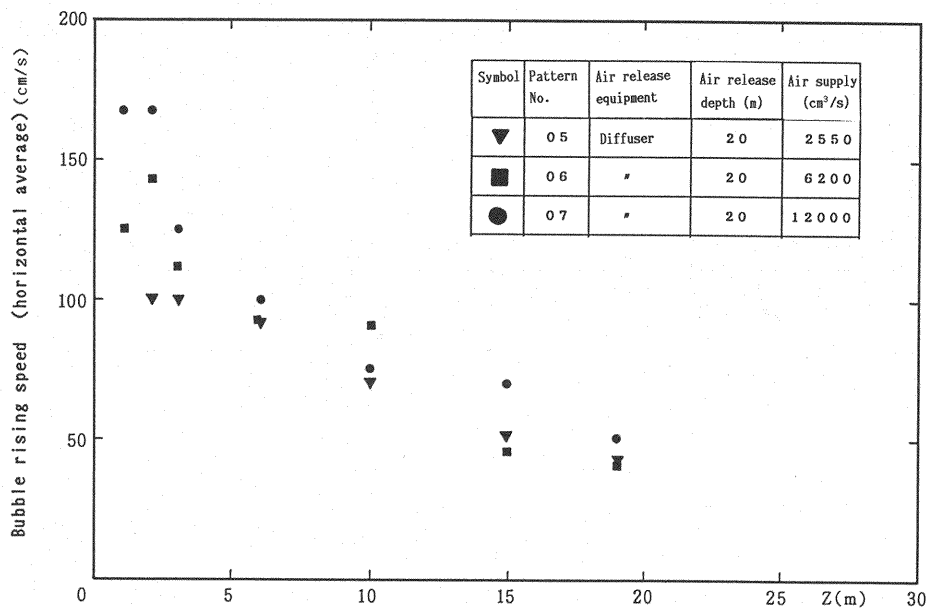
Symbol	Pattern No.	Air release equipment	Air release depth (m)	Air supply (cm³/s)
▼	0 5	Diffuser	2 0	2 5 5 0
■	0 6	"	2 0	6 2 0 0
●	0 7	"	2 0	1 2 0 0 0

Fig. 6   Vertical distribution of bubble velocity

Regression curve
$$W_a = 11.3\, Q_a^{atm\ 1/4}\,(cm/s)$$

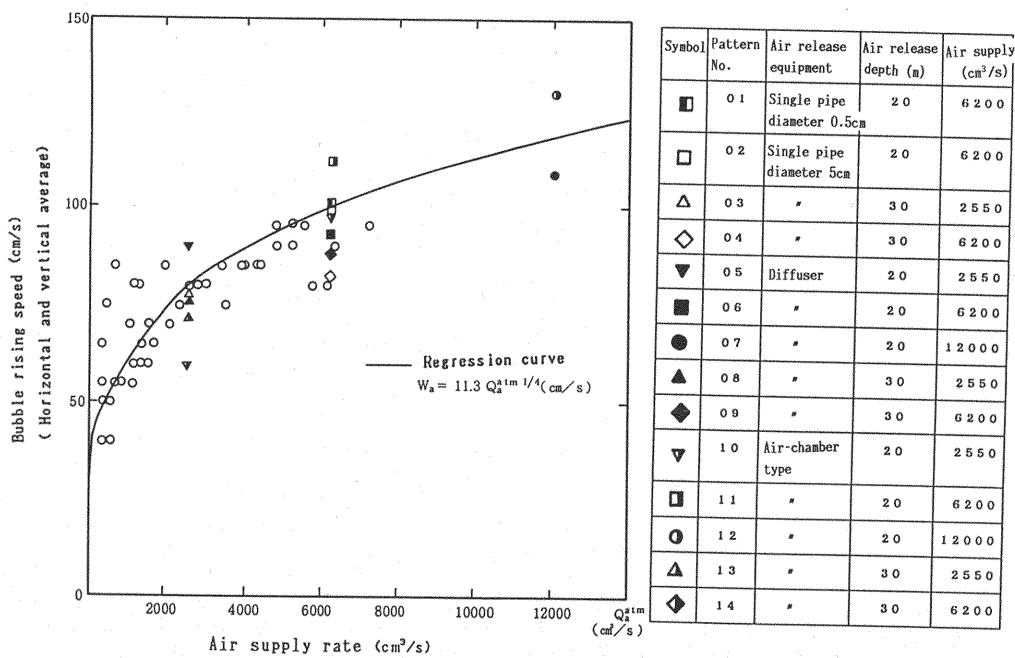| Symbol	Pattern No.	Air release equipment	Air release depth (m)	Air supply (cm³/s)
▥	0 1	Single pipe diameter 0.5cm	2 0	6 2 0 0
▢	0 2	Single pipe diameter 5cm	2 0	6 2 0 0
△	0 3	"	3 0	2 5 5 0
◇	0 4	"	3 0	6 2 0 0
▼	0 5	Diffuser	2 0	2 5 5 0
■	0 6	"	2 0	6 2 0 0
●	0 7	"	2 0	1 2 0 0 0
▲	0 8	"	3 0	2 5 5 0
◆	0 9	"	3 0	6 2 0 0
▽	1 0	Air-chamber type	2 0	2 5 5 0
▥	1 1	"	2 0	6 2 0 0
◑	1 2	"	2 0	1 2 0 0 0
△	1 3	"	3 0	2 5 5 0
◈	1 4	"	3 0	6 2 0 0

Fig. 7   Relationship between bubble rising speed and air supply rate
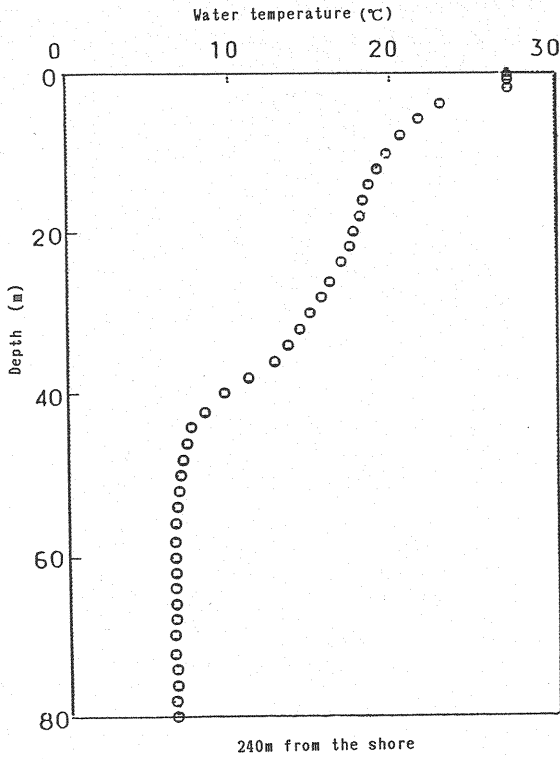
Fig. 8 Vertical distribution of temperature (before experiment)
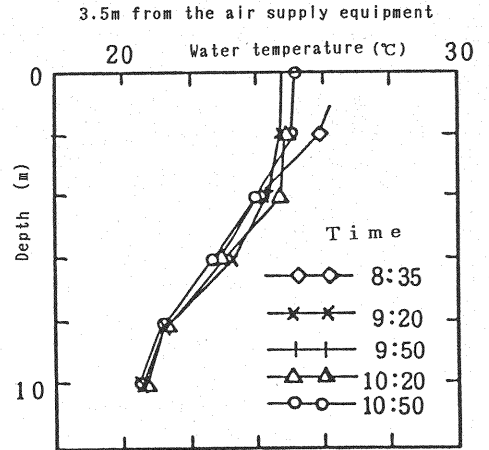
3.5m from the air supply equipment
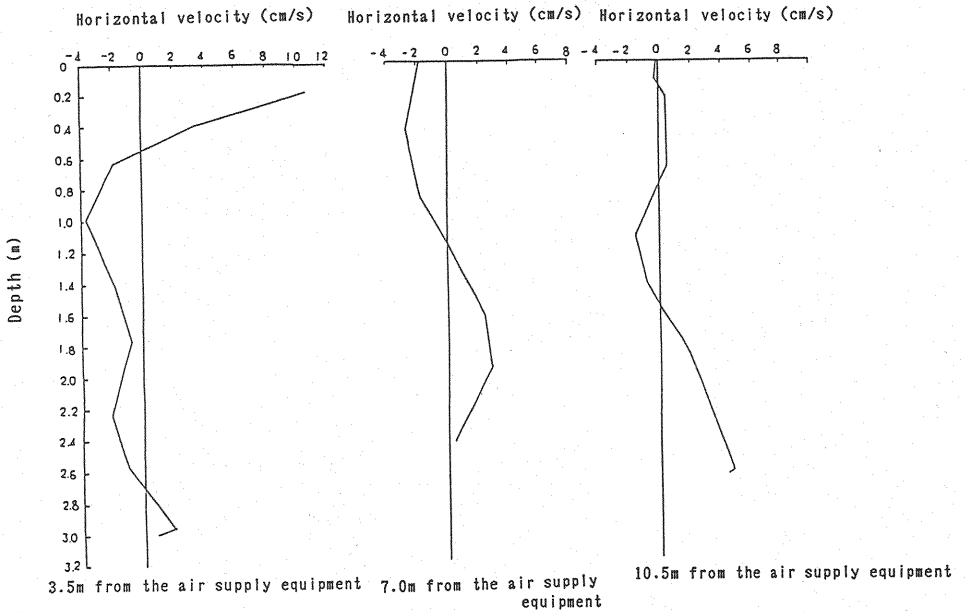
Fig. 9 Vertical distribution of temperature (under experiment)

Fig. 10 Vertical distribution of horizontal velocity (Single pipe diamter is 0.5cm, Depth is 20m, Air supply rate is 6200cm^3/s)
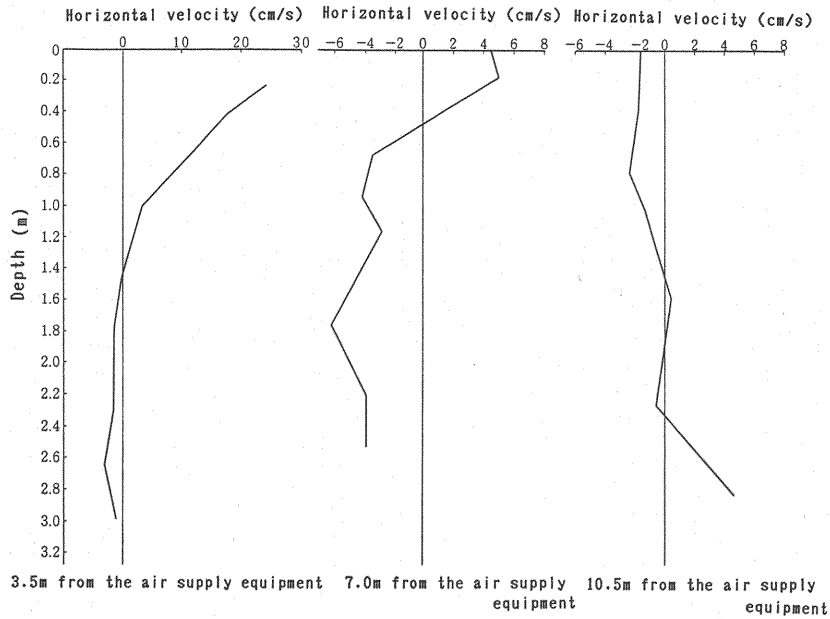
Horizontal velocity (cm/s)   Horizontal velocity (cm/s)   Horizontal velocity (cm/s)

Fig. 11   Vertical distribution of horizontal velocity
(Air chamber type, Depth is 20m, Air supply rate is
$12000cm^3/s$)

3.5m from the air supply equipment   7.0m from the air supply   10.5m from the air supply
equipment   equipment

$b_{0.5}$
$\lambda b_{0.5}$
$\mu b_{0.5}$
(cm)

——o—— $b_{0.5}$ (half width of profile of plume velocity)
---●--- $\lambda b_{0.5}$(half width of air bubble)
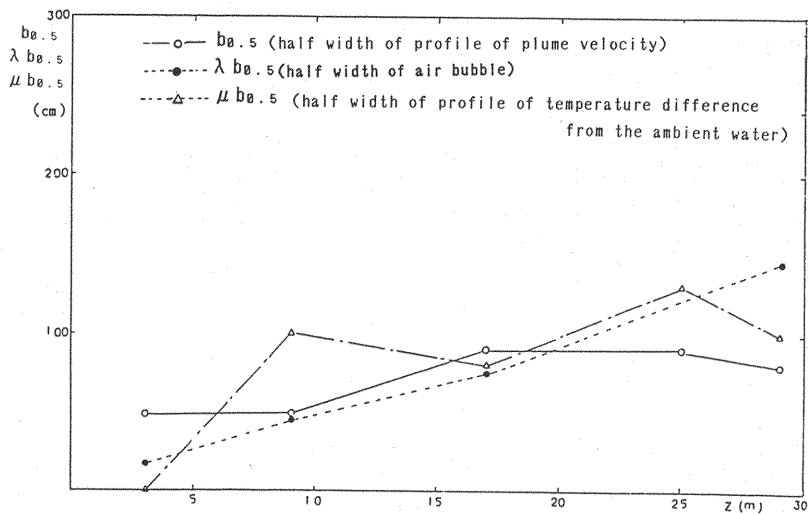---△--- $\mu b_{0.5}$ (half width of profile of temperature difference
from the ambient water)

Fig. 12   Half width of air bubble plume
(Single pipe diameter is 5cm, Depth is 30m,
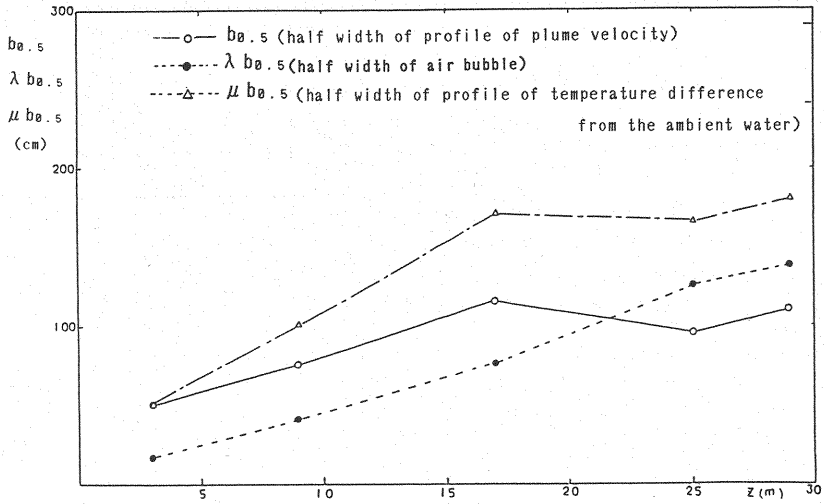Air supply rate is $6200cm^3/s$)

Fig. 13 Half width of air bubble plume
(Diffuser, Depth is 30m,
Air supply rate is 6200cm^3/s)

temperature difference from the ambient water are shown in Figs. 12 and 13. The
half width of air bubbles increases with the bubble rise and reaches a maximum
value at the water surface. The half widths of profiles of plume velocity and
temperature difference have low rates of increase with height above the air outlet
and show maximum values considerably below the water surface in several cases.

The integration of the velocity around the axis of the plume, are shown in
the form of non-dimensional volume flux in Figs. 14~18. Note that the volume flux
at the water surface are calculated from the horizontal velocity distribution near
the bubble column. These figures show that the increase of the volume flux and
its non-dimensional form are considerably different depending on the experimental
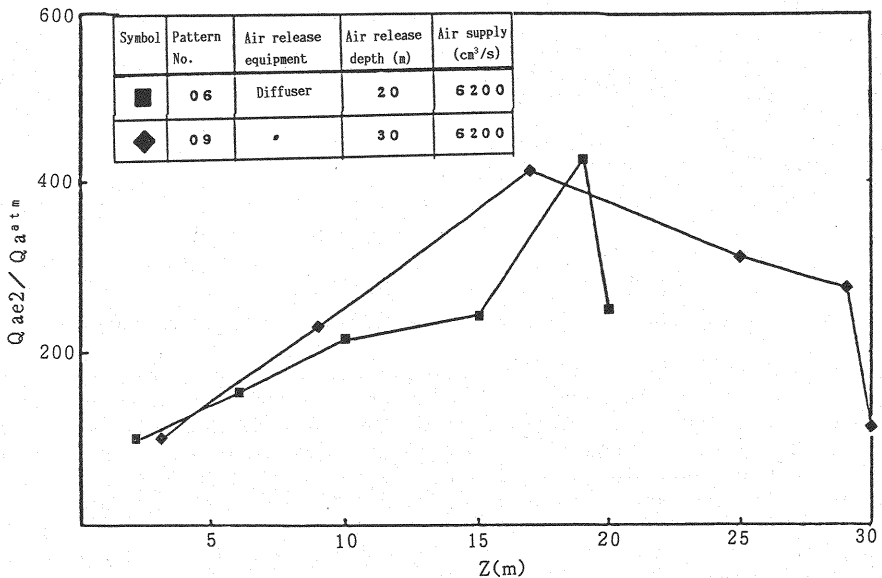condition of air release depth and air supply rate. Figure 14 shows change in

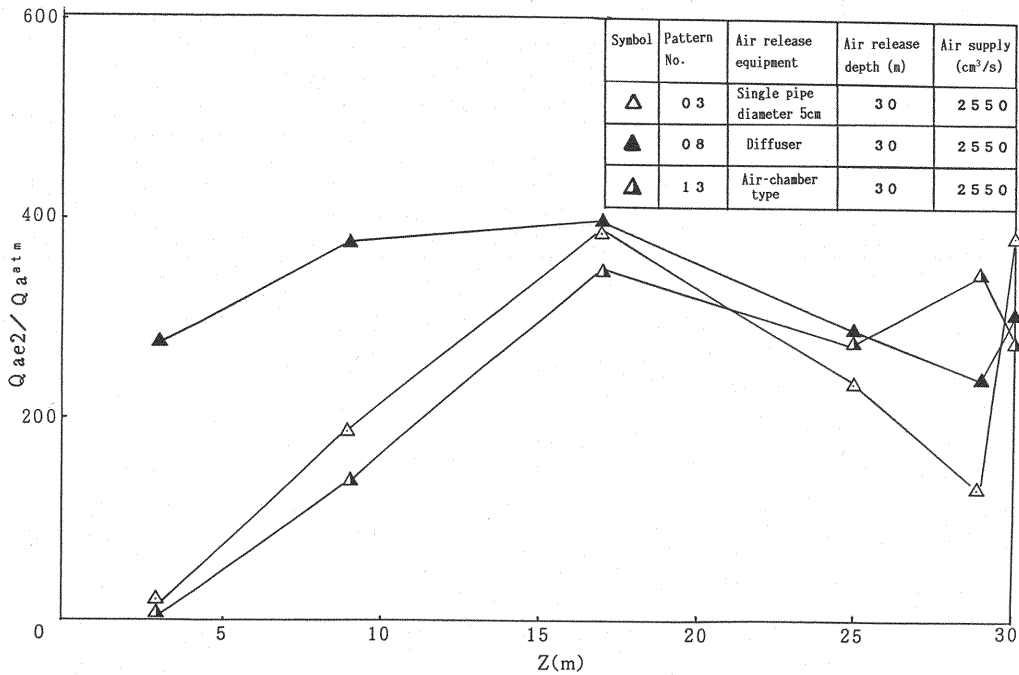Fig. 14 Volume flux ratio (Change with depth)

Symbol	Pattern No.	Air release equipment	Air release depth (m)	Air supply (cm³/s)
△	0 3	Single pipe diameter 5cm	3 0	2 5 5 0
▲	0 8	Diffuser	3 0	2 5 5 0
△	1 3	Air-chamber type	3 0	2 5 5 0

Fig. 15   Volume flux ratio (Change with air supply equipment)

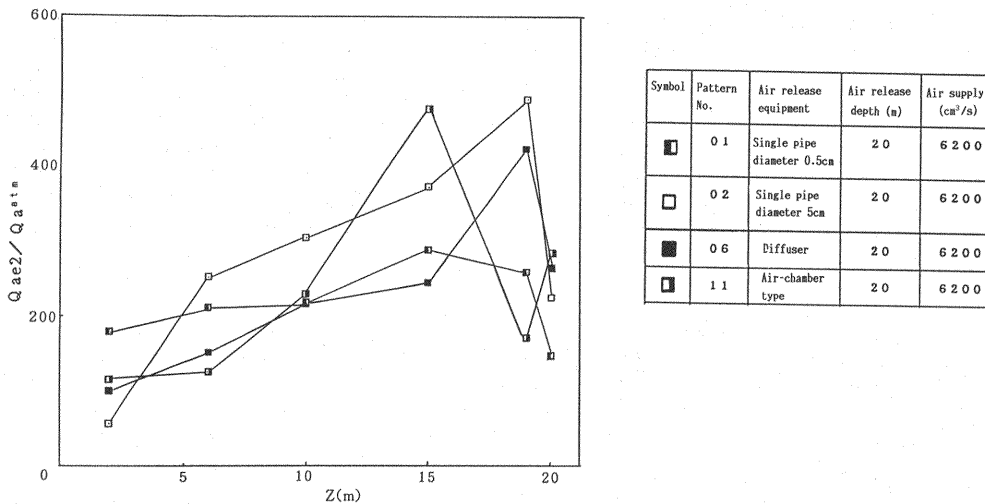| Symbol	Pattern No.	Air release equipment	Air release depth (m)	Air supply (cm³/s)
▣	0 1	Single pipe diameter 0.5cm	2 0	6 2 0 0
□	0 2	Single pipe diameter 5cm	2 0	6 2 0 0
▩	0 6	Diffuser	2 0	6 2 0 0
▢	1 1	Air-chamber type	2 0	6 2 0 0

Fig. 16   Volume flux ratio (Change with air supply equipment)

volume flux ratio with depth. The volume flux ratio reaches a maximum value
before the flow reaches the water surface in the case of 30m injection, and not
in the case of 20m injection. This is caused by the stratification of the ambient
water. Figures 15 and 16 show changes in volume flux ratio with the type of air
release equipment. There is no significant difference in the volume flux ratio
between three types of equipment : diffuser, single pipe and air chamber type.
Figures 17 and 18 show that the ambient water entrained by air bubble plume does
not always reach the water surface according to the condition of air supply rate
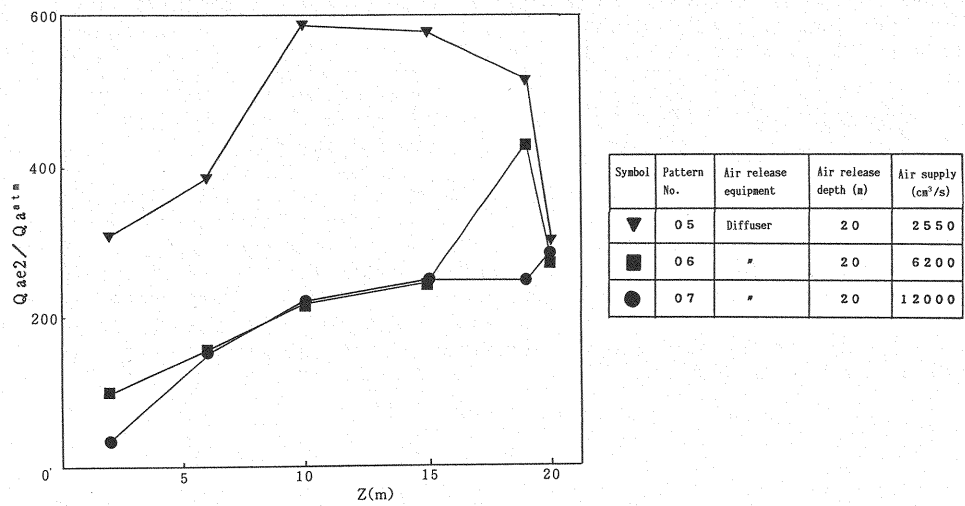and air release depth.

Symbol	Pattern No.	Air release equipment	Air release depth (m)	Air supply (cm³/s)
▼	0 5	Diffuser	2 0	2 5 5 0
■	0 6	〃	2 0	6 2 0 0
●	0 7	〃	2 0	1 2 0 0 0

Fig. 17 Volume flux ratio (Change with the rate of air supply)

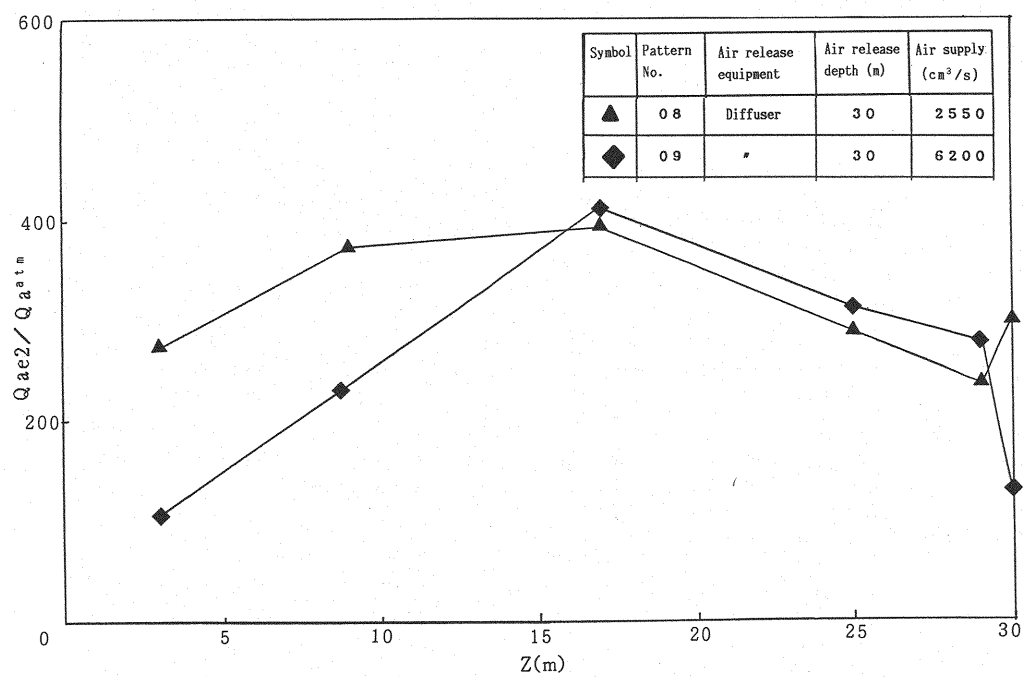| Symbol	Pattern No.	Air release equipment	Air release depth (m)	Air supply (cm³/s)
▲	0 8	Diffuser	3 0	2 5 5 0
◆	0 9	〃	3 0	6 2 0 0

Fig. 18 Volume flux ratio (Change with the rate of air supply)

These measured volume flux ratio can be approximated by the following equation obtained from an integral theory for bubble plumes in a homogeneous environment (3) as shown in Fig. 19.

$$\frac{Qae_2}{Q_a^{atm}} = \frac{f}{F_1}, \quad \frac{1}{F_1} \equiv \sqrt{A_1 \frac{\rho - \rho_a}{\rho} g \int_0^Z \frac{Patm/(Wac\ Q_a^{atm})}{Patm + \rho g\ (H_2 - z)}\ dz} \quad (4)$$

In the figure, solid line represents theoretical values calculated from equation (4) and plots experimental data with the same definition of symbols as in Fig. 7. The data in Fig. 19 are classified into two groups : 1) sufficient mixing in which the entrained water reaches the water surface and 2) insufficient mixing in which the entrained water does not reach the water surface owing to the stratification, and compared with the theory in Fig. 20. The theory overestimates the insufficient mixing data and maximum value of the volume flux ratio exists. This maximum value is 500~600.
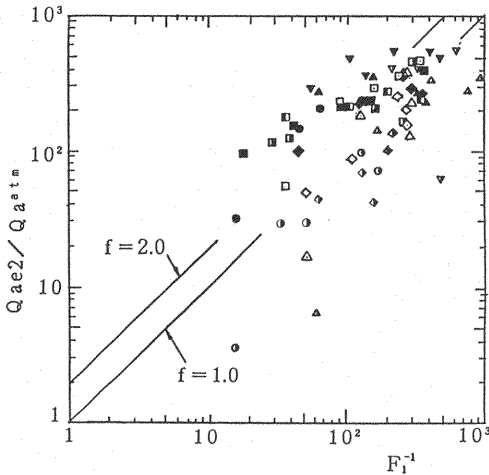

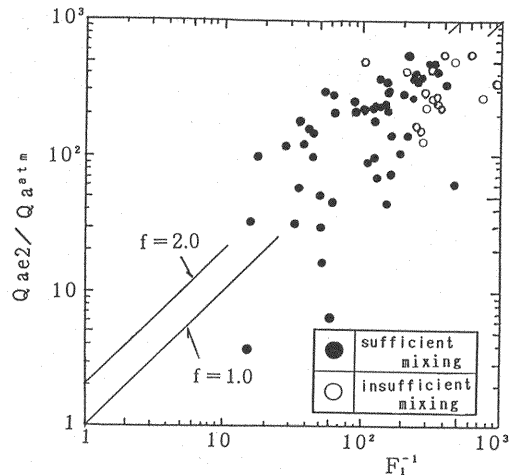Fig. 19 Theoretical and experimental values of volume flux ratio

Fig. 20 Volume flux ratio and mixing pattern

CONCLUSION

1. Bubble rising speed which is needed for the calculation of entrainment flux
    by air bubble plume can be estimated by the theory based on the balance of
    buoyancy and drag force exerted on a single bubble for small air supply rate.
    However, for large air supply rate, the theory cannot be applied and an
    empirical formula is proposed based on the experimental data of the authors
    and Kobus.
2. Entrainment flux by air bubble plume is approximately estimated from an
    integral theory for bubble plumes in a homogeneous environment. However, the
    ambient water entrained by air bubble plume does not always reach the water
    surface according to the condition of air supply rate and air release depth.

REFERENCES

1. Kobus, H.E. : Analysis of the flow induced by air-bubble system, Proc.11th
    Conference on Coastal Engineering, 1968, pp.1016-1031.
2. J. Matsumoto and M. Nakamura : Experimental studies on the behavior and
    characteristics of air bubbles from a single orifice, Proc. of JSCE, No.260,
    1977 (in Japanese).
3. S. Matsunashi and Y. Miyanaga : Basic Study of Air Bubble Plume used for
    Measure against Water Quality, CRIEPI, Report No.U87066, 1988 (in Japanese).
4. S. Matsunashi and Y. Miyanaga : The Application of Simulation Model for Flow
    induced by Air Bubble Plume in Thermally Stratified Reservoirs, CRIEPI,
    Report No.U88029, 1988 (in Japanese)
5. Y. Miyanaga and S. Matsunashi : Effects of Hydraulic Measures for Reservoir
    Eutrophication, CRIEPI, Report No.U88066, 1988 (in Japanese).
6. T. Tadaki and S. Maeda : On the shape and velocity of single air bubbles
    rising in various liquids, Chem. Eng. 25, 1961 (in Japanese).

APPENDIX - NOTATIONS

The following symbols are used in this paper:

Re	= Reynolds number of bubbles;
d	= bubble diameter;
Wa	= bubble rising speed;
ν	= kinematic viscosity;
Cd	= drag coefficient;
Q_a^{atm}	= air supply rates under the atmospheric pressure;
$Qae2$	= Volume flux entrained by air-bubble plume;
f	= distribution coefficient;
A_1	= cross sectional area;
$\rho, \rho a$	= water and air density;
$Patm$	= atmospheric pressure;
Wac	= bubble rising speed on the central axis of the plume; and
H_2	= air release depth.